Journal of Power Sources 196 (2011) 8519–8524

Contents lists available at ScienceDirect

Journal of Power Sources

journal homepage: www.elsevier.com/locate/jpowsour

Cell performance of polymer electrolyte fuel cell with urchin-like carbon supports

Juei Dong Lu, Ming-Chang Yang*

Department of Chemical Engineering, National Cheng Kung University, Tainan 701, Taiwan

ARTICLE INFO

Article history:
Received 26 April 2011
Received in revised form 8 June 2011
Accepted 9 June 2011
Available online 16 June 2011

Keywords:
Polymer electrolyte fuel cell
Urchin-like carbon support
Mesoporous carbon
Carbon nanotube
Cell performance

ABSTRACT

Urchin-like structured carbon comprising carbon nanotubes grown on Fe catalyst-seeded mesoporous carbon have shown promising results as catalyst supports for use in direct methanol fuel cells (DMFCs) and proton exchange membrane fuel cells (PEMFCs). The Fe catalyst is prepared on the mesoporous carbon by immersion process followed by a high temperature reduction. The growth of carbon nanotubes then progress, for a predetermined time, through the thermal decomposition of acetylene at 800 °C. The resulting structure, comprising intimately connected mesoporous carbon and carbon nanotubes, is shown to offer performance advantages as a catalytic support for DMFCs and PEMFCs. When the hot-pressing pressure is fixed 20 kg cm^{-2} to fabricate a membrane electrode assembly (MEA) with urchin-like carbon supports, the CNT growth time is found to be 60 min for a highest maximum power density in both DMFCs and PEMFCs. The maximum power densities are 43 and 79% higher than those with purely mesoporous carbon in DMFCs and PEMFCs, respectively. In a direct comparison with commercial E-TEK catalyst, the urchin-like catalyst shows higher maximum power densities, in DMFC and PEMFC, by approximately 17 and 31%, respectively.

1. Introduction

In recent years, low temperature fuel cells, such as proton exchange membrane fuel cells (PEMFCs) and direct methanol fuel cells (DMFCs) have attracted much interest due to their potential for applications in portable electronic devices and transportation. However, the commercialization of fuel cell technology is still confronted by some major challenges, such as the catalytic activity for oxygen reduction and methanol oxidation. The application of new catalytic materials with high activity and good stability will play a key role in the improvement of fuel cell performance.

In order to improve catalytic activity and utilization, carbon materials with highly electrical conductivities and chemical stabilities have been used as catalytic supports for fuel cells. In the past, several carbon materials have been synthesized as electrocatalyst supports for fuel cells [1–8]. The nature and structure of the carbon supports can also affect critical characteristics, such as the mass transport [8] and electronic conductivity [3], of the catalytic layer and the activity of the catalytic metal [4,6]. Hence, the fabrication of carbon supports with optimized morphological characteristics is very important in fuel cell applications.

Mesoporous carbon with a high surface area, high pore volume and tunable pore structure was synthesized with a silica template to achieve, both: a high catalytic dispersion, and the efficient diffusion of reactants [7]. Compared to commercial Vulcan XC-72 carbon, mesoporous carbon (with pore diameters in the range 2–50 nm) affords a high degree of catalyst utilization by improving the entrapment of Pt catalyst in its micropores (<2 nm diameter). Yu et al. [8] and Chai et al. [9] reported that mesoporous carbon, for use in DMFCs, can be synthesized to have a larger pore volume and a higher surface area, resulting in a higher catalyst dispersion and a higher methanol diffusion rate. Mesoporous carbon, with an optimal pore diameter of 25 nm, showed the highest maximum power density, which was 43% higher than a commercial catalyst; however, poor interfacial contact within the mesoporous carbon in catalytic layer resulted in a large electrical resistance. To reduce the contact resistance within the carbon supports, an appropriate amount of bare carbon nanotubes (CNTs), or carbon nanotubes with Pt–Ru (Pt–Ru/CNTs), were mixed with mesoporous catalysts (Pt–Ru/MC) [10]. Interestingly, the catalysts made with 80 wt.% Pt–Ru/MC and 20 wt.% Pt–Ru/CNTs showed a higher electrocatalytic activity than the E-TEK catalyst used under the same conditions. This result indicated that the CNTs were an idea additive for electrode to improve the electrocatalytic activity.

This study aimed to improve the performance of the catalysts in DMFCs and PEMFCs by growing the carbon nanotubes on mesoporous carbon, using catalytic chemical vapor deposition (CVD) to form urchin-like mesoporous carbon as a catalytic support. CNTs were known to be highly conductive along their axial direction. In the application of electric double-layer capacitors (EDLCs), the improvement in electronic conductivity of a carbon cloth electrode by grafting the CNTs on the fiber surface of the cloth has been confirmed [11,12]. In a previous report, the obtained CNTs adhered to

* Corresponding author. Tel.: +866 6 275 7575x62666; fax: +886 6 234 4496.
E-mail address: mcyang@mail.ncku.edu.tw (M.-C. Yang).

0378-7753/$ – see front matter © 2011 Elsevier B.V. All rights reserved.
doi:10.1016/j.jpowsour.2011.06.041

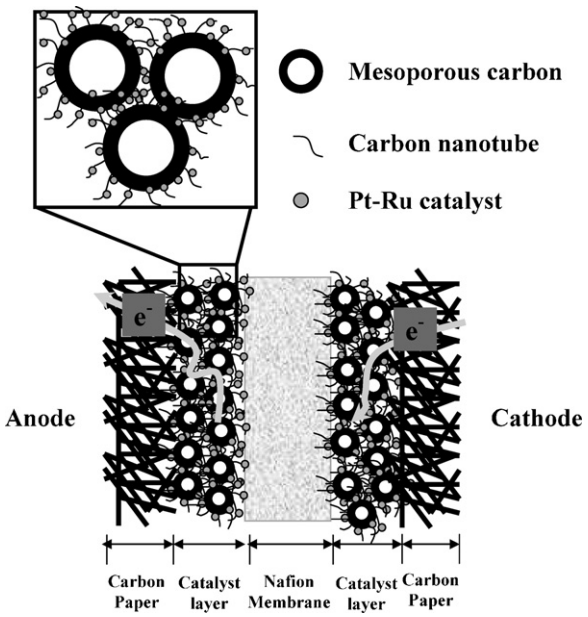

Fig. 1. Schematic representation of the electron transport within a catalytic layer in a MEA. The inset shows how the CNTs improve the conductivity between mesoporous carbon.

the mesoporous carbon with intimate contact resulted in a network which was composed of CNTs and mesoporous carbon [13]. Both the high inherent electrical conductivity of the CNTs and their intimate contact with the carbon supports, as shown in Fig. 1, were factors expected to enhance electrical conductivity within the catalytic layer when the urchin-like carbon supports were used in DMFC and PEMFC applications. An additionally factor expected to augment the electrochemical activity and catalytic ability, is the presence of defect sites; especially, edge-plane sites, previously shown to be present on the CNT surface [5]. In this report, the cell performances, when using urchin-like carbon, as a catalyst support, have been evaluated with DMFCs and PEMFCs.

2. Experimental

The mesoporous carbon was prepared according to a previous report [14]. In brief, a defined ratio of phenol formaldehyde (PF) and polyethylene oxide (PEO) was mixed to form a miscible polymer blend, which aggregated with silicate to form a PF–PEO–silica composite with the pH being controlled in the range from 4.0 to 5.0. Mesoporous carbon was obtained through pyrolysis of the PF–PEO–silica composite, under a nitrogen atmosphere, and after HF-etching of silicate. After which, the CNTs were grown, using Fe as a catalyst, on mesoporous carbon by chemical vapor deposition. The mesoporous carbon was first immersed in aqueous $Fe(NO_3)_3$ (0.037 M) at room temperature for 24 h. The mesoporous carbon was then separated from the solution by filtration and was dried in air at 60 °C overnight. The iron precursor-containing carbon was placed in a tubular furnace and then reduced in H_2 at 600 °C for 1 h. Subsequently, the furnace temperature was raised to 800 °C for CNT growth, with a 1% C_2H_2/Ar mixture being used as the feed gas. The growth time was controlled in the range 5–120 min.

In this report, well dispersed Pt–Ru nanoparticles were prepared by a micro-emulsion method. Two reverse micellar solutions were prepared, using sodium bis(2-ethylhexyl)sulfosuccinate (AOT, Alfa Aesar) and cyclohexane as a surfactant and an oil phase, respectively. In both solutions, the volume ratio of the aqueous phase and the oil phase was 1:24.7. The molar ratio of water and AOT was 10:1 in the aqueous phase with AOT being present 0.225 M in oil phase. The first micro-emulsion solution was prepared by mixing chloroplatinic acid ($H_2PtCl_6{\cdot}6H_2O$, Acors), ruthenium chloride ($RuCl_3$, Stem), D.I. water, AOT, and cyclohexane with ultrasonic agitation for 30 min. An appropriate amount of carbon support was then added into the stirred solution to ensure a metal (Pt–Ru) loading of 20 wt.% on carbon. The Pt:Ru atomic ratio in this solution was 1:1. The second micro-emulsion solution contained sodium borohydride ($NaBH_4$) in sodium hydroxide solution, AOT and cyclohexane at pH 11. After being stirred separately for 2 h, these two solutions were mixed under constant stirring for another 2 h. The catalyst/conjugates namely: Vulcam XC-72 carbon (Pt–Ru/XC-72), mesoporous carbon (Pt–Ru/MC) and urchin-like carbon (Pt–Ru/MC–CNT) were obtained after filtration and washing with ethanol, acetone and D.I. water, with final drying in air at 60 °C.

The carbon supports and the catalysts were analyzed by scanning electron microscopy (SEM, JSM-6700F, JEOL) and transmission electron microscopy (TEM, FE-2000, Hitachi). The total surface areas and pore volumes of the carbon supports were determined by applying the Brunauer–Emmett–Teller (BET, ASAP2000, Micromeritics) equation in N_2 adsorption/desorption. X-Ray diffractometry (XRD, D/MAX, RIGAKU) was carried out with a Cu-K_α source at room temperature. The average grain size of the platinum metal particles was calculated from the Debye–Scherrer equation using the most distinct peak, Pt (1 1 1) around $2\theta = 39.7^\circ$, fitted by a Gaussian function. The atomic composition of Pt–Ru catalysts was evaluated by an energy-dispersive X-ray spectrometer (EDX) which was attached to the SEM.

Catalytic ink was prepared by mixing the catalysts, D.I. water and Nafion solution (5 wt.%), at a carbon/dry Nafion ratio of 7:3, and a Nafion solution/water ratio of 1:1, in an ultrasonic bath for 30 min and then stirring for 2 h. Then the catalytic ink was brushed on wet-proofed carbon papers (TGPH-060, Toray) with Pt loadings of 1.2 mg cm^{-2} and 0.8 mg cm^{-2} to form the anode and cathode, respectively, in the DMFC system, while in the PEMFC system the Pt loading was 0.8 mg cm^{-2} for both electrodes. The active geometrical areas of the single cells were 1.8 cm × 1.8 cm and 2.5 cm × 2.5 cm for the DMFCs and the PEMFCs, respectively. The anodes and cathodes were hot pressed (135 °C for 1.5 min) on both sides of a Nafion 117 membrane (Dupont) to form a membrane electrode assembly (MEA).

Cell polarization curves were obtained using an electronic load (model 63010 from Chroma). For the DMFCs, methanol (3 M) at 65 °C and oxygen at 60 °C were fed to the anodes and cathodes, respectively. For the PEMFCs, hydrogen at 95 °C and oxygen at 70 °C were fed to anodes and cathodes, respectively. The cell temperatures were held at 80 °C and 70 °C for the DMFCs and PEMFCs, respectively, throughout the experiments.

3. Results and discussion

SEM images of mesoporous carbon with CNTs, grown for various times, show that the length of the CNTs increased with the growth time, as shown in Fig. 2. When the growth time was more than 30 min, the CNTs grew significantly longer and became twisted and entwined around the mesoporous carbon, so that estimating the length of the CNTs became difficult. In this study, Fe, as the catalyst, was located at the tip of a growing CNT, as shown in Fig. 3. The CNTs were in the tip growth mode and presented a bamboo-like structure. Fig. 3 shows the CNTs sitting on the mesoporous carbon, indicating the generation of an intimate contact region, between CNTs and the mesoporous carbon. Such intimate contacts, and the interconnections of CNTs, among mesoporous carbon have been proved to improve the electrical conduction between the mesoporous carbon supports [13].

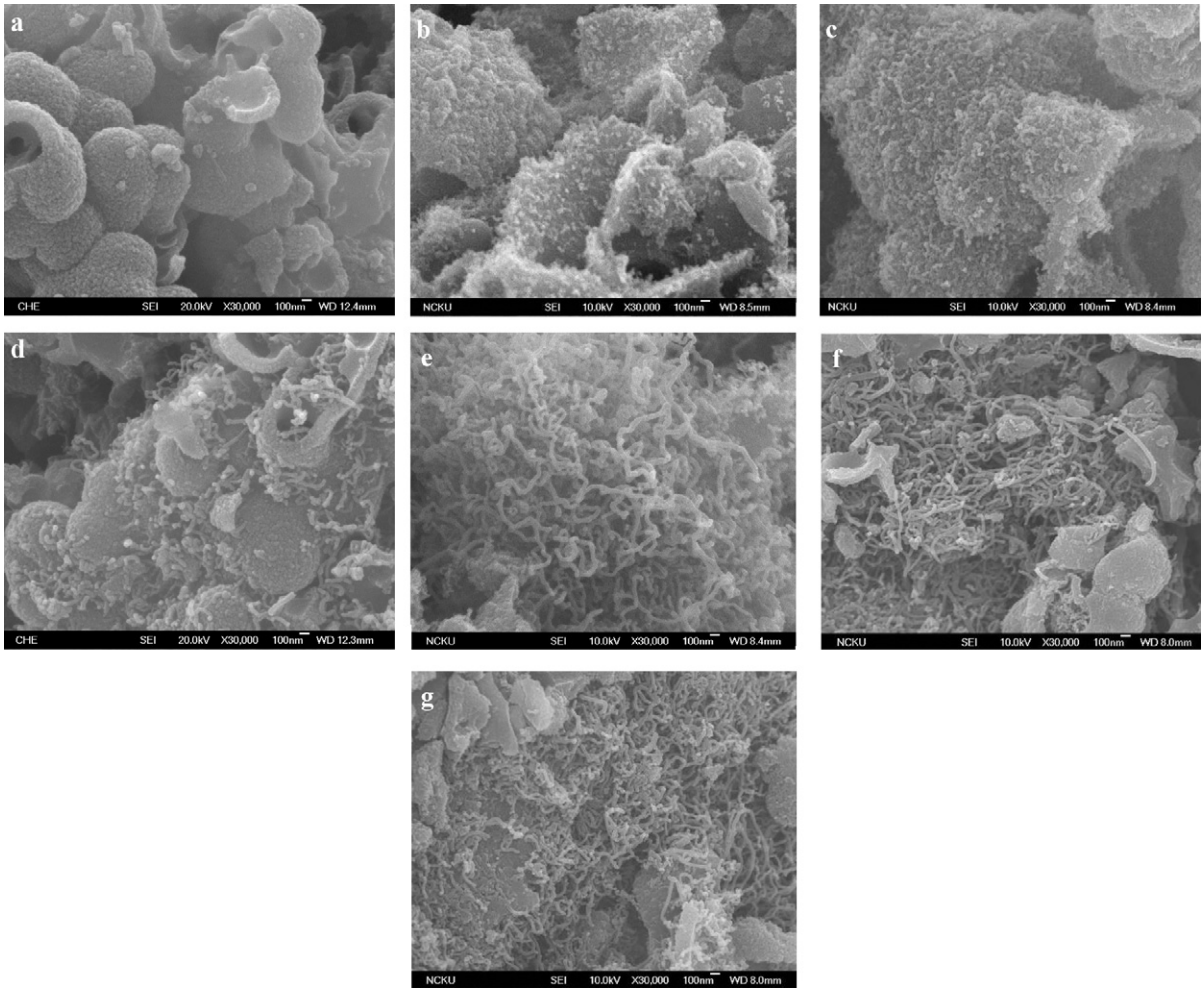

Fig. 2. SEM images of (a) mesoporous carbon and urchin-like mesoporous carbon with growth times of (b) 5, (c) 15, (d) 30, (e) 60, (f) 90, and (g) 120 min.

Table 1 reveals the BET surface areas, pore diameters and pore volumes of various types of carbon supports. The number in bracket of each sample designates the growth time of CNTs on mesoporous carbon. The commercial carbon support, Vulcam XC-72, had the smallest surface area and pore volume, 243 $m^2\ g^{-1}$ and 0.4 $cm^3\ g^{-1}$, respectively. It was also noticeable that the BET surface area and the pore volume of urchin-like carbon decreased with CNT growth time. In a previous report, the decrease in the BET surface area and the pore volume have been attributed to blockage of the pores by CNTs and by pyrolytic carbon particles [13]. Table 2 shows the Pt–Ru content, atomic ratio, grain sizes and particle sizes of the Pt–Ru catalysts on various carbon supports. The Pt–Ru contents in all catalysts, prepared by micro-emulsion method, were less than the nominate value, 27.5 wt.%. This might be due to some metal loss during impregnation. It shows that the atomic ratios of Ru/Pt on various types of carbon supports were close to the nominate value (Ru/Pt = 1), same as the commercial E-TEK catalyst. Additionally, the average sizes of all Pt–Ru catalysts were similar to that of E-TEK catalyst.

Fig. 4 shows the cell performances with Pt–Ru catalysts deposited on mesoporous and urchin-like carbons with various CNT growth times. All the MEA were prepared by hot-pressing with a

Table 1
Structure parameters of carbon supports.

Type of carbon support	CNT growth time (min)	S_{BET} ($m^2\ g^{-1}$)	Pore diameter (nm)	Pore volume ($cm^3\ g^{-1}$)
MC	–	820	3.7	1.1
MC–CNT (5)	5	792	3.7	1.1
MC–CNT (15)	15	743	3.8	1.0
MC–CNT (30)	30	688	3.7	1.0
MC–CNT (60)	60	635	3.7	0.9
MC–CNT (90)	90	582	3.7	0.8
MC–CNT (120)	120	524	3.7	0.8

Table 2
Characteristics of Pt–Ru catalysts on various types of carbon supports.

Type of catalyst	Nominal Pt–Ru content (wt.%)	Pt–Ru content from TGA (wt.%)	Atomic ratio of Ru/Pt[a] from EDX	Grain size from XRD (nm)	Particle size from TEM (nm)
MC	27.5	24.8	0.96	3.7	2.8
MC–CNT (60)	27.5	20.1	1.02	2.9	3.1
Vulcum XC-72	27.5	23.6	1.05	3.5	3.2
E-TEK	20.0	22.2	1.03	3.6	3.2

[a] Nominal atomic ratio of Ru/Pt = 1.

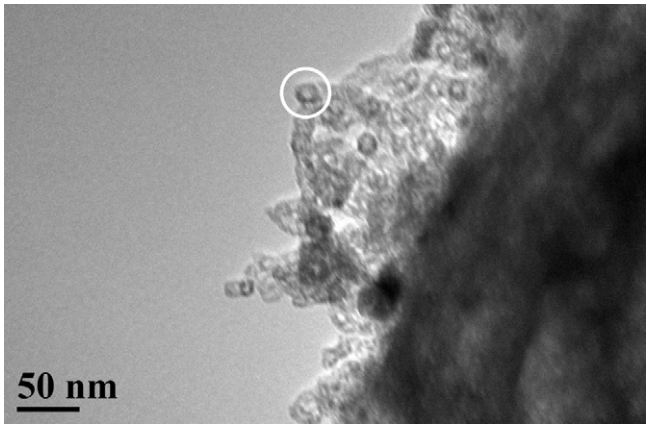

Fig. 3. TEM image of CNTs on the mesoporous carbon. Fe catalysts at the tip of a CNT.

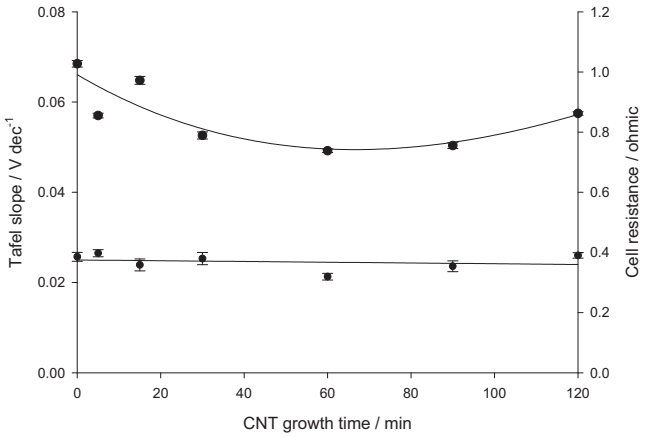

Fig. 5. Tafel slope (●) and resistances (▲) of cells with urchin-like catalysts as functions of CNT growth time. The growth time of 0 min is for mesoporous catalyst.

pressure of 20 kg cm^{-2}. The maximum power densities were 18.1, 18.2, 18.8, 21.1, 21.5 and 16.7 mW cm^{-2} for the urchin-like carbon formed with CNT growth times of 5, 15, 30, 60, 90 and 120 min, respectively. All of these measured power densities are higher than the 15 mW cm^{-2} for the mesoporous carbon. The CNT growth on the mesoporous carbon increased the maximum power density up to 43%. It was experimentally determined that time in the order of 60–90 min were appropriate for CNT growth to give optimal, i.e., larger maximum power densities. When the CNT growth time reached 120 min, the cell performance degraded significantly.

From the polarization curve, the: Tafel slope (b), and the cell resistance (R) can be obtained by fitting the: cell potential (E), and the current (i), with the semi-empirical equation [15]:

$$E = E^0 - b \quad \log \quad i - iR \tag{1}$$

This equation does not apply for the high current region where flooding occurs and E^0 can be expressed by:

$$E^0 = E_r - b \quad \log \quad i_0 \tag{2}$$

where E_r and i_0 are the reversible potential and the exchange current. The Tafel slope is a kinetic parameter of both oxygen reduction and methanol oxidation. The cell resistance is contributed by: proton resistance (electrolyte), electron resistance (electrode) and mass transport resistance (reactants). In this report, the proton resistance in MEA was made to be as uniform as possible by fabricating the electrodes with constant Nafion content within the anodes and cathodes of all the MEAs; thus allowing for the direct comparison of results. Therefore, the resistance difference observed in the experiments can be attributed to the electron and mass transport resistances in both the anode and the cathode. The Tafel slope and the cell resistance with Pt–Ru/MC–CNT depended on the CNT growth time as shown in Fig. 5. There was no significant difference in Tafel slope between these catalysts, thus the catalyst activity could be considered constant. Fig. 5 also shows that the cell resistance with the Pt–Ru/MC–CNT decreased when the CNT growth time increased to 60 min. The cell resistance with Pt–Ru/MC was about 1.03 Ω which is higher than 0.74 Ω found with Pt–Ru/MC–CNT (60), i.e., the cell resistance decreased by 28% with the CNT growth. However, when the CNT growth time was more than 90 min, the cell resistance was found to increase. There are two plausible explanations for this resistance increase: the twisting and entwining of CNTs around the mesoporous carbon prohibited the transport of reactants, such as methanol, or alternatively the pores in the mesoporous carbon facilitating the effective transport of reactants were blocked by CNTs and pyrolytic carbon particles particularly with extended growth times. The electrical conductivity was enhanced by growing the CNTs on mesoporous carbon, albeit at the price of increasing the mass transport resistance within the electrode. The urchin-like carbon with the CNTs growth time of 60 min gave the best cell performance.

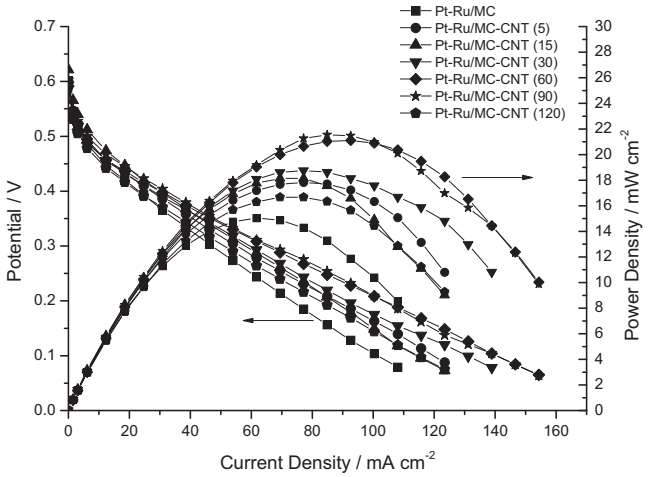

Fig. 4. Effect of CNT growth time on the polarization curve and power density of DMFC with PtRu catalysts deposited on mesoporous carbons and urchin-like carbons.

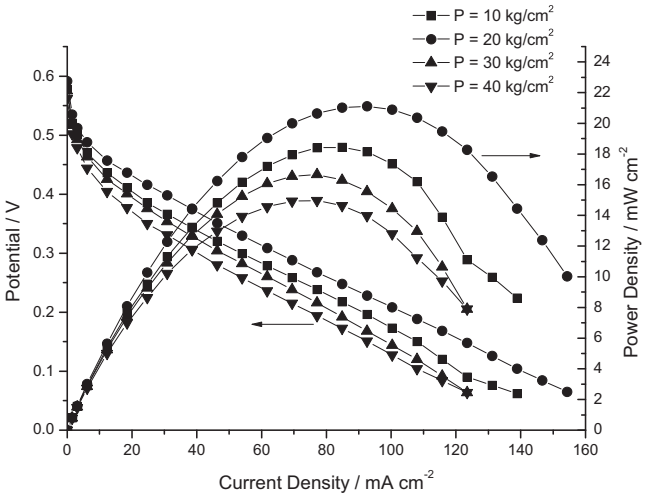

Fig. 6. Effect of hot-pressing pressure on the polarization curve and power density of DMFC with PtRu–MC–CNT (60) catalyst.

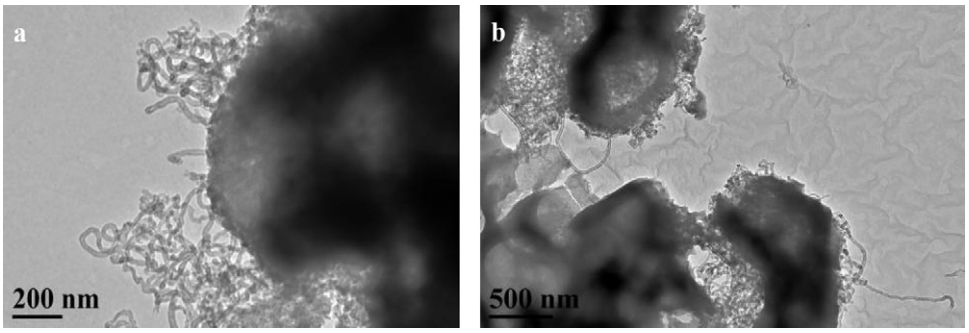

Fig. 7. TEM images of urchin-like catalyst after hot-pressing at (a) 20 kg cm^{-2} and (b) 30 kg cm^{-2}.

Fig. 6 shows the polarization curves and the power densities of a DMFC for the electrodes made of Pt–Ru/MC–CNT (60) catalysts at various hot-pressing pressures in MEA fabrication. The best cell performance was obtained at 20 kg cm^{-2} hot-pressing pressure. When the hot-pressing pressure was larger than 20 kg cm^{-2}, the cell performances decay significantly possible due to structural damage of the carbon supports, which ruptured at high hot-pressing pressures, as shown in Fig. 7. It is believed that the structural integrity of urchin-like carbons can provide a pathway facilitating the effective transport of electrons and reactants by nanotubes and mesoporous carbon, respectively, in DMFC.

Fig. 8 shows the comparative cell performance of DMFCs with Pt–Ru catalysts deposited on Vulcan XC-72 and urchin-like carbon supports for anodes and cathodes, in comparison to similar cells using E-TEK catalysts. The open-circuit voltages were 0.592, 0.545 and 0.565 V for Pt–Ru/MC–CNT (60), Pt–Ru/XC-72 and E-TEK catalysts, respectively. The corresponding maximum power densities were 21.1, 16.5 and 18 mW cm^{-2}. The urchin-like catalysts, Pt–Ru/MC–CNT (60), gave a higher maximum power density than the Pt–Ru/XC-72 and the E-TEK catalysts by about 28 and 17%, respectively. The improved cell performance with urchin-like catalysts appears to result from high open-circuit voltages, high activity and low cell resistance. The improvement in the cell performance with the urchin-like catalysts was also observed in PEMFCs, as shown in Fig. 9. The urchin-like catalyst, Pt–Ru/MC–CNT (60), revealed higher maximum power density than Pt–Ru/MC–CNT (30), and much higher than Pt–Ru/MC, similar result with that in DMFCs. The maximum power density for Pt–Ru/MC–CNT (60) was 203 mW cm^{-2}, compared with 113 and 155 mW cm^{-2} for Pt–Ru/MC and E-TEK catalyst, respectively: corresponding to increases in the maximum power densities of 79 and 31%, respectively. It was believed that the excellent performance of the PEMFC with the urchin-like carbon support could be attributed to the low electrical resistance and specific structure of the urchin-like carbon, which facilitated the efficient diffusion of reaction gases. Comparing Figs. 8 and 9, it is apparent that the improvement in the performance of the PEMFC was higher than for the DMFC.

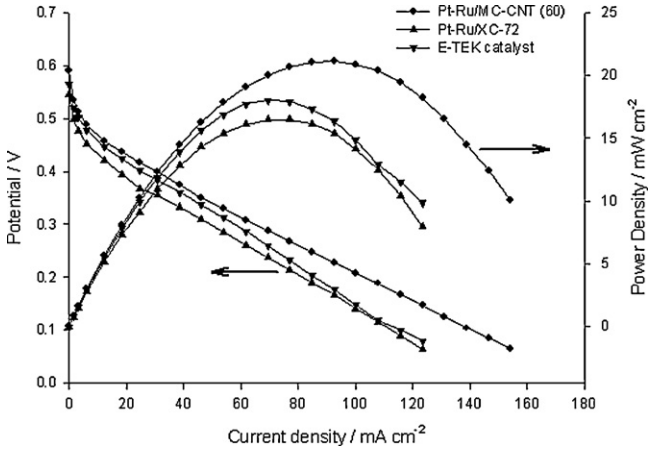

Fig. 8. Polarization curves and power density of DMFC with E-TEK catalyst and Pt–Ru catalyst deposited on XC-72 and urchin-like carbon.

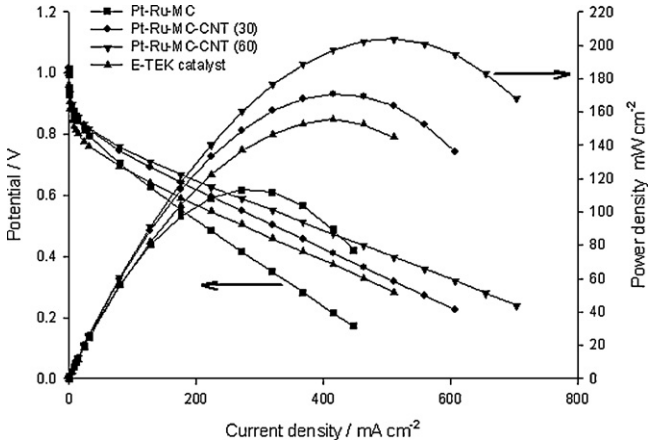

Fig. 9. Polarization curves and power density of PEMFC with E-TEK catalyst and Pt–Ru catalyst deposited on mesoporous and urchin-like carbon.

4. Conclusions

Urchin-like carbon, prepared by growing the CNTs on mesoporous carbons with catalytic chemical vapor deposition technique, was successfully used as a catalyst support for DMFCs and PEMFCs. The length of the CNTs on mesoporous carbons increased with the CNT growth time, while the surface area and the pore volume diminished. All the urchin-like carbons supported Pt–Ru catalysts exhibited higher maximum power density than the mesoporous carbons without CNTs. The urchin-like carbon with the CNTs growth time of 60 min gave the best cell performance. The significant decrease of the resistance was attributed to the existence of the CNTs on mesoporous carbon providing pathways for electron transfer. Furthermore, the urchin-like catalysts have better interconnections and a stable catalytic structure within the electrode at a hot-pressing pressure of 20 kg cm^{-2} during MEA fabrication. The maximum power densities with urchin-like carbon support were larger than those with mesoporous carbon support by approximately 43 and 79% in DMFC and PEMFC, respectively. Similarly, the maximum power densities with urchin-like carbon support were larger than those with E-TEK catalyst by 17 and 31% in the DMFC and PEMFC, respectively.

Acknowledgements

The authors wish to acknowledge the financial support from the National Science Council in Taiwan under grant NSC-95-2120-M-006-009. Special thank should go to Professor Hung-Shan Weng in the Department of Chemical Engineering for fundamental discussion on catalyst and Professor Hong-Ping Lin in the Department of Chemistry for providing the mesoporous carbon. An appreciation also should go to Ms. Mei-Her Chen for her technical helps.

References

[1] S. Tang, G. Sun, J. Qi, S. Sun, J. Guo, Q. Xin, G.M. Haarberg, Chin. J. Catal. 31 (2010) 12–17.
[2] H. Liu, C. Song, L. Zhang, J. Zhang, H. Wang, D. Wilkinson, J. Power Sources 155 (2006) 95–110.
[3] X. Sun, R. Li, D. Villers, J.P. Dodelet, S. Desilets, Chem. Phys. Lett. 379 (2003) 99–104.
[4] Z. Lei, M. Zhao, L. Dang, L. An, M. Lu, A.-Y. Lo, N. Yu, S.-B. Liu, J. Mater. Chem. 19 (2009) 5985–5995.
[5] Y. Piao, K. An, J. Kim, T. Yu, T. Hyeon, J. Mater. Chem. 16 (2006) 2984–2989.
[6] G. Wu, D.Y. Li, C.S. Dai, D.L. Wang, N. Li, Langmuir 24 (2008) 3566–3575.
[7] V. Raghuveer, A. Manthiram, Electrochem. Solid State Lett. 7 (2004) A336–A339.
[8] J.S. Yu, S. Kang, S.B. Yoon, G. Chai, J. Am. Chem. Soc. 124 (2002) 9382–9383.
[9] G.S. Chai, S.B. Yoon, J.S. Yu, J.H. Choi, Y.E. Sung, J. Phys. Chem. B 108 (2004) 7074–7079.
[10] C.F. Chi, M.C. Yang, H.S. Weng, J. Power Sources 193 (2009) 462–469.
[11] H. Zhang, G.P. Cao, Y.S. Yang, Z.N. Gu, J. Electrochem. Soc. 155 (2008) K19–K22.
[12] C.W. Huang, H.S. Teng, J. Electrochem. Soc. 155 (2008) A739–A744.
[13] C. Chuang, S. Sharma, J. Ting, H. Lin, H. Teng, C. Huang, Diam. Relat. Mat. 17 (2008) 606–610.
[14] C.Y. Chang-Chien, C.H. Hsu, H.P. Lin, C.Y. Tang, C.Y. Lin, J. Porous Mat. 13 (2006) 195–199.
[15] E.A. Ticianelli, C.R. Derouin, A. Redondo, S. Srinivasan, J. Electrochem. Soc. 135 (1988) 2209–2214.